01 Oct 1996

Generation of Synthetic-Focus Images from Pulse-Echo Ultrasound using Difference Equations

Daryl G. Beetner
Missouri University of Science and Technology, daryl@mst.edu

R. Martin Arthur

Recommended Citation

D. G. Beetner and R. M. Arthur, "Generation of Synthetic-Focus Images from Pulse-Echo Ultrasound using Difference Equations," *IEEE Transactions on Medical Imaging*, vol. 15, no. 5, pp. 665-672, Institute of Electrical and Electronics Engineers (IEEE), Oct 1996.
The definitive version is available at https://doi.org/10.1109/42.538944

Generation of Synthetic-Focus Images from Pulse-Echo Ultrasound Using Difference Equations

Daryl G. Beetner and R. Martin Arthur,* *Member, IEEE*

Abstract— **To produce a complete-dataset, pulse-echo image requires a knowledge of the time of flight (TOF) from each source to each sensor in the transducer array for each site to be imaged. Increasing the speed of TOF calculation is important in adaptive-focus schemes. We determined TOF more rapidly than via direct calculation by representing TOF surfaces by two-dimensional (2-D), positive-integer-degree polynomials implemented in their forward-difference form. Errors which accumulate due to the use of a difference equation depend on the degree of the polynomial and on the size of the image. The number of bits needed to address echo samples in backscatter memory and the allowable error define the minimum precision needed for accurate values of TOF. Accurate calculation of TOF, expressed as 10-b addresses in backscatter memory, for each pixel in a 512×512 image with a second-degree difference equation requires 44 b of precision. Using the complete dataset from a 32-element array and a second-degree approximation to TOF on a typical graphics workstation reduced generation time of a 512×512 image from 702 to 239 s. Parallel formulation of both the TOF calculation and the retrieval and summation of echo samples resulted in significant further reduction in image-generation time. Parallel implementation on a SIMD array with 4096 processors, each of which had an indirect-addressing mode, allowed the generation of a 512×512 image in 16.3 s.**

I. Introduction

BOTH FOCUS-and-steer images and synthetic-focus images, made with the complete dataset from pulse-echo ultrasonic systems that have N-element transducers, contain the effect of averaging samples from N^2 backscattered signals at each pixel in the image [1]–[3]. Because synthetic-focus techniques separate data acquisition from image generation, images can be produced from the same backscattered signals under different assumptions about the nature of the medium being imaged and with different focus modes. Thus adaptive-focus schemes can be used to generate synthetic-focus images without the need to reacquire backscattered signals.

To focus requires taking into account the time of flight (TOF) from the radiation source to the location in the insonified medium corresponding to each image pixel and from each pixel to the sensor [4]. For a rectangular coordinate display, the location of each pixel must be converted to cylindrical coordinates, an operation that requires finding the square root of a sum of squares. Thus, the direct computation of TOF at each pixel over N^2 surfaces can be time consuming. In an adaptive-focus scheme new TOF surfaces must be found for each source-sensor pair each time an image is formed.

TOF is determined by the geometry of the transducer array in relation to the image region and by the average speed of sound along the path from source to the site of interest and back to the sensor. If the image region and the speed of sound are fixed, then TOF surfaces need to be calculated only once and may be retrieved from memory more rapidly than they can be calculated. If, however, the image region changes, or more importantly, if synthetic-focus images are generated iteratively to improve image quality or to extract estimates of speed of sound, then TOF surfaces change at each iteration. Previously, we systematically varied the assumed speed of sound used to produce synthetic-focus images from a single dataset to find the speed of sound which maximized image energy [5]. Thus, efficient computation of TOF surfaces with an appropriate model may be critical both for 1) improving image quality by providing a nearly exact focus at each pixel and 2) characterizing tissue by extracting estimates of the variation in the speed of sound over the tissue region [6].

Work previously reported from this laboratory described an approach for generating real-time, synthetic-focus images in which each pixel in the image is in focus [7]. We approximated the TOF surface with a two-dimensional polynomial containing positive, integer powers of azimuth and range. This polynomial, which is in rectangular coordinates, allows convenient generation of a raster scan display. In its forward-difference form, it can be updated in the time it takes to perform a single addition. Truncating the polynomial at the second degree in both azimuth and range produced a TOF approximation which was consistently and significantly better than a paraxial approximation [8]. The coefficients of this polynomial can be found from numeric evaluation over rectangular regions or found via an analytic expression over sector-shaped regions [9].

Although using a difference equation can reduce the time needed to calculate TOF, the implementation of a polynomial approximation to TOF as a difference equation can introduce another source of error. Here we characterize the errors that result from the repeated application of difference equations. These errors determine the precision or number of bits which must be used in the calculation of a difference equation to insure accurate results. We also describe algorithms for synthetic-focus image generation on both serial and parallel

Manuscript received November 21, 1994; revised April 29, 1996. The Associate Editor responsible for coordinating the review of this paper and recommending its publication was R. Martin. *Asterisk indicates corresponding author.*

D. G. Beetner is with the Electronic Systems and Signals Research Laboratory, Department of Electrical Engineering, Washington University, St. Louis, MO 63130 USA.

*R. M. Arthur is with the Electronic Systems and Signals Research Laboratory, Department of Electrical Engineering, Washington University, St. Louis, MO 63130 USA (e-mail: rma@ee.wustl.edu).

Publisher Item Identifier S 0278-0062(96)07483-6.

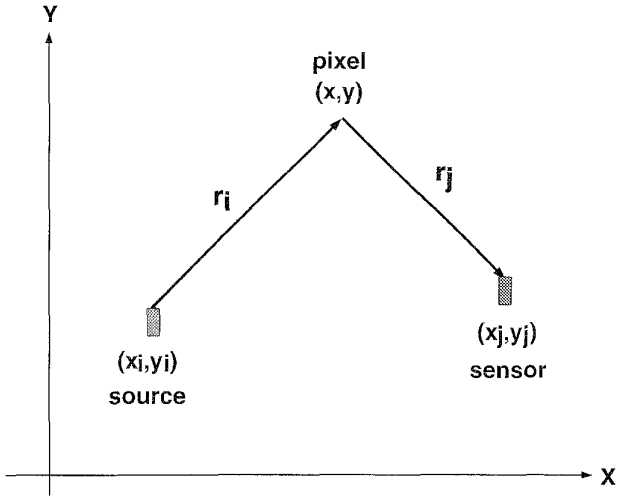

Fig. 1. Determination of TOF for arbitrary source, sensor, and pixel locations. TOF is given by the path length from the source to the location in the medium corresponding to the pixel (r_i) divided by the average speed of sound along $\boldsymbol{r}_i$ plus the path length from the pixel to the sensor (r_j) divided by the average speed of sound along $\boldsymbol{r}_j$.

machines based on the use of difference equations to represent TOF.

II. Synthetic-Focus Image Generation

Synthetic-focus image generation from pulse-echo ultrasound using the complete dataset is based on ellipsoidal backprojection of backscattered signals acquired for each source-sensor pair in a transducer array [4]. The geometry of the array is arbitrary. The geometry of a single source-sensor pair in relation to a single site in the image region is shown in Fig. 1. Reconstruction to yield an estimate of the scattering potential for a particular site in an image region consists of the following steps in the spatial-temporal domain.

1) Weight each backscattered signal by $r_i r_j / r^2$ for each site, where the radii describe the reconstruction site.
2) Backproject the weighted backscattered signal to the reconstruction site.
3) Average the weighted backprojections from all source-sensor pairs.

Our algorithm is the same as point-focus imaging using either focus-and-steer beamforming or synthetic-focus reconstruction with the complete dataset except for the $r_i r_j / r^2$ weighting factor, which is necessary to conserve energy [4]. This factor is significant only if the image region is at a range comparable to or less than the size of the transducer array.

III. Representation of Time-of-Flight Surfaces

Image generation from backscattered energy requires mapping scattered signals to image locations consistent with their arrival times at the sensor, i.e., their TOF's from source to sensor. TOF is

$$t_{\text{of}}(x,y) = \frac{r_i + r_j}{c_o} \tag{1}$$

where c_o is the average speed of sound or background velocity of the medium and,

$$r_i = \sqrt{(x - x_i)^2 + (y - y_i)^2} \tag{2a}$$

$$r_j = \sqrt{(x - x_j)^2 + (y - y_j)^2}. \tag{2b}$$

The source is located at (x_i, y_i), the focal point at (x, y), and the sensor at (x_j, y_j), as illustrated in Fig. 1.

We represent the TOF surface by a power series approximation of degree N and M in the x and y directions, respectively

$$f(x,y) = \sum_{k=0}^{N} \sum_{l=0}^{M} a_{k,l} x^k y^l. \tag{3}$$

This approximation to a TOF surface, $f(x, y)$, is usually scaled to yield the address in memory of the sampled backscattered signal corresponding to a desired TOF. Computation of the coefficients $a_{k,l}$ which describe a region characterized by a fixed speed of sound may be performed numerically or analytically [9]. If the average speed of sound along a given path is not known, then TOF can be found by using the polynomial itself. Coefficients of the polynomial can be estimated based on maximizing appropriate properties of iteratively formed images. An important property of the polynomial is that it may be evaluated at any point along an arbitrary contour in a single-addition time using either a forward-difference or backward-difference implementation.

IV. Implementation of Difference Equations

Because the polynomial $f(x, y)$ possesses positive-integer powers of x and y, it can be formulated as a stable forward-difference equation. In general, $(N+1)$ $(M+1)$ forward difference terms describe a polynomial whose highest degree in x is N and in y is M. Terms beyond the Nth difference in x and the Mth difference in y are identically zero.

The forward-difference terms are determined by evaluating the polynomial about some reference point (x_o, y_o) within its region of support. Because we scan each TOF surface in a raster fashion, azimuth and range coordinates were scaled so that step size was 1. In this case the first, second, and third forward differences in one dimension are

$$\Delta_x^1 f(x_o, y_o) = f(x_o + 1, y_o) - f(x_o, y_o) \tag{4a}$$

$$\Delta_x^2 f(x_o, y_o) = f(x_o + 2, y_o) - 2f(x_o + 1, y_o) + f(x_o, y_o) \tag{4b}$$

$$\Delta_x^3 f(x_o, y_o) = f(x_o + 3, y_o) - 3f(x_o + 2, y_o) + 3f(x_o + 1, y_o) - f(x_o, y_o). \tag{4c}$$

The magnitudes of the coefficients associated with each of the terms in the finite-difference expansion form Pascal's triangle.

In general, the forward differences at (x_o, y_o) are [10], [11]

$$\Delta_x^n \Delta_y^m f(x_o, y_o) = \sum_{k=0}^{n} \sum_{l=0}^{m} (-1)^{n+m-k-l} \cdot \binom{n}{k} \binom{m}{l} f(x_o + k, y_o + l) \tag{5}$$

where

$$\binom{n}{k} = \frac{n!}{k!(n-k)!}. \tag{6}$$

The polynomial can be evaluated at any displacement (k, l) from (x_o, y_o) using the difference coefficients determined at (x_o, y_o) because

$$f(x_o + k, y_o + l) = \sum_{n=0}^{k} \sum_{m=0}^{l} \binom{k}{n} \binom{l}{m} \Delta_x^n \Delta_x^m f(x_o, y_o). \tag{7}$$

The maximum values for n and m are N and M, the degree of the polynomial in x and y, respectively. Thus, because higher-order differences are zero, a second-degree polynomial in x and y with $l = 0$ contains only three terms

$$f(x_o + k, y_o) = f(x_o, y_o) + \binom{k}{1} \Delta_x^1 f(x_o, y_o) + \binom{k}{2} \Delta_x^2 f(x_o, y_o). \tag{8}$$

In a raster scan, the difference coefficients at any site can be found recursively from the values at (x_o, y_o), so that $f(x_o + k, y_o)$ can be found from the difference terms at $(x_o + k - 1, y_o)$. Thus

$$f(x_o + k, y_o) = f(x_o + k - 1, y_o) + \Delta_x^1 f(x_o + k - 1, y_o) \tag{9}$$

where

$$\Delta_x^1 f(x_o + k - 1, y_o) = \Delta_x^1 f(x_o + k - 2, y_o) + \Delta_x^2 f(x_o + k - 2, y_o) \tag{10a}$$

and

$$\Delta_x^2 f(x_o + k - 2, y_o) = \Delta_x^2 f(x_o + k - 3, y_o) = \Delta_x^2 f(x_o, y_o). \tag{10b}$$

Note that the second difference term does not change. It remains constant because it is updated by the third difference, which for a second-degree difference equation is identically zero. We previously described a recursive structure for implementing the general, two-dimensional approximation to a TOF surface, (7), in which all of the additions for generating new TOF values along a contour may be performed in parallel [7]. A new value of TOF can be produced in the time of a single addition using this recursive structure.

V. Accuracy of Difference Equations

If TOF is found using a difference equation in order to minimize the time needed to compute a TOF surface, errors in the coefficients at the initial site in the image (x_o, y_o) are propagated to the result at subsequent sites. Coefficient errors at the initial site and the number of times the coefficients must be updated (determined by the size of the image) decide the precision needed to produce a TOF value with a sufficient number of error-free significant bits, i.e., the number of bits needed to specify the addresses of echo signals in backscatter memory.

A. Error Production by Difference Equations

The errors initially present in the difference coefficients can propagate through many bits with the use of a difference equation over images of the size typically encountered in medical ultrasonic imaging. Error is propagated as the result of performing multiple additions. The lower the order of a difference coefficient, the farther its error propagates. This fact is demonstrated by (9) and (10). The highest-order coefficient does not change. The result itself, which has the lowest order (order zero), is affected by more additions than any other coefficient.

The only arithmetic operation required to implement (7) is addition. The error in the result of an addition is the sum of the errors in the addends, assuming that the result is not truncated or rounded. We assumed that the only error in the difference coefficients at the initial site (x_o, y_o) was quantization error.

The error of interest here is the error which accumulates through the recursive use of the difference coefficients at (x_o, y_o), i.e., the error in using (7). Therefore

$$\text{Error}\,[f(x_o + k, y_o + l)] = \text{Error}\left[\sum_{n=0}^{k} \sum_{m=0}^{l} \binom{k}{n} \binom{l}{m} \Delta_x^n \Delta_x^m f(x_o, y_o)\right]. \tag{11}$$

Because the combination factors are integer terms which introduce no error themselves, the error in the TOF at $(x_o + k, y_o + l)$ is the quantization error in the difference terms at (x_o, y_o) propagated by the use of the difference equation

$$\text{Error}\,[f(x_o + k, y_o + l)] = \sum_{n=0}^{k} \sum_{m=0}^{l} \binom{k}{n} \binom{l}{m} \text{Error}\,[\Delta_x^n \Delta_x^m f(x_o, y_o)]. \tag{12}$$

The actual error at any displacement (k, l) depends on the initial errors of the difference coefficients. We are, however, not interested in the actual error itself, but in how many bits of precision must be used to specify the error after stepping through all the pixels in the image. We assumed that the error in the result of the summations in (12) is the sum of the absolute values of the errors in the addends and that the summation is neither truncated nor rounded.

Without further loss of generality, we can bound the error-propagation distance by assuming that all the initial difference coefficients are represented by integers with a quantization error of one, i.e., the least-significant bit is in error. With all the errors at (x_o, y_o) equal to one, the error at $(x_o + k, y_o + l)$ measures how far the error in the least-significant bit at (x_o, y_o) propagates. Thus

$$[\text{propagation distance}]_{\text{bits}} \leq \log_2 \left[\sum_{n=0}^{N} \sum_{m=0}^{M} \binom{K}{n} \binom{L}{m}\right] \tag{13}$$

where K and L are the sizes of the image in x and y directions, and N and M are the degrees of the polynomial approximation to TOF in the x and y directions, respectively. In the imaging situations of interest, $K \gg N$ and $L \gg M$. In this case,

TABLE I
BOUNDS ON DIFFERENCE-EQUATION PRECISION
REGISTER LENGTHS IN BITS FOR 10 B OF ACCURACY
DIFFERENCE EQUATIONS OF DEGREES ONE TO FOUR IN BOTH AZIMUTH AND RANGE

Image Size	Degree 1	Degree 2	Degree 3	Degree 4
128x128	24	36	47	57
256x256	26	40	53	65
512x512	28	44	59	73
1024x1024	30	48	65	81

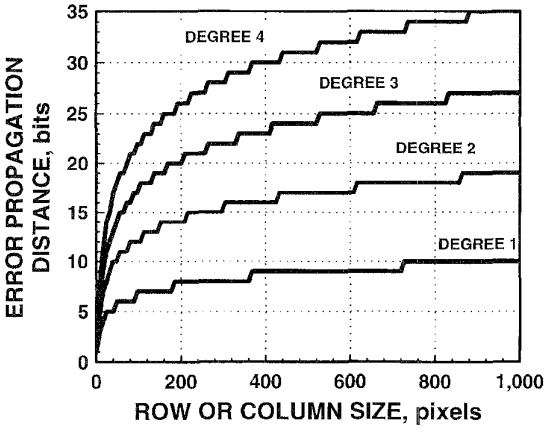

Fig. 2. Propagation of the error from one end of a row or column in an image to the other with the use of a difference equation. The error propagates farther and, therefore, requires more bits to specify as the degree of the difference equation is increased.

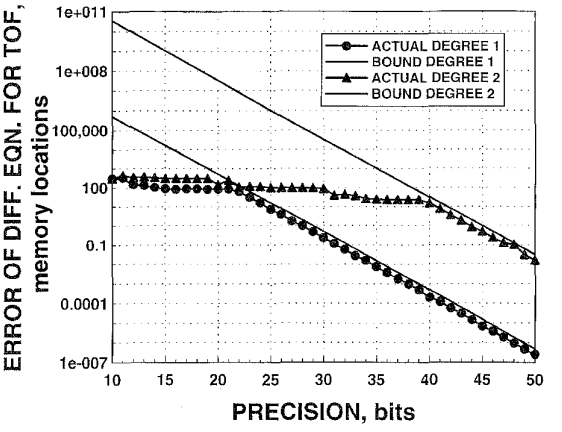

Fig. 3. Errors produced by using difference equations to describe TOF over a 512×512 image. Backscattered signals were assumed to be sampled at 50 MHz, so that adjacent memory locations contained samples separated by the sample interval, 20 ns. The 30×30 mm image region was at a minimum range of 70 mm. The transducer contained 32 elements separated by 1.4 mm. Worst-case experimental error and the theoretical error bound for a first-degree difference equation of TOF (lower curve and bound). Worst-case experimental error and the theoretical error bound for a second-degree difference equation of TOF (upper curve and bound).

the propagation distance is dominated by the last term in the double summation

$$[\text{propagation distance}]_{\text{bits}} \leq \log_2 \left[\binom{K}{N} \binom{L}{M} \right], \quad \text{for} \quad K \gg N \quad \text{and} \quad L \gg M. \tag{14}$$

Because the expression for the propagation distance is separable, it can be described by characterizing its behavior over a row or column of an image. Fig. 2 depicts the propagation distance over rows or columns of up to 1000 pixels for first-degree through fourth-degree polynomials. Clearly, the propagation distance rises steeply from the initial site of application of the difference equation then levels off at row or column sizes that depend on the degree of the TOF polynomial.

B. Numerical Precision of Difference Equations

To prevent the quantization error in the initial difference coefficients from affecting the desired TOF result at other pixels in an image, the number of bits of precision in the representation of TOF must be set both to accommodate the desired accuracy and to allow for the propagation of the quantization error. Thus

$$[\text{precision}]_{\text{bits}} = [\text{accuracy}]_{\text{bits}} + [\text{propagation distance}]_{\text{bits}}. \tag{15}$$

Table I lists the precision required to produce ten accurate bits over square images using first- to fourth-degree polynomials. For the conditions in Table I, the results using the double summation in (13) and the approximation to that double summation (14) are identical.

Our expressions for the required precision of difference equations assume that the maximum amount of error is generated from every arithmetic operation. In practice, the errors could be much less, so that register lengths smaller than those predicted could be used. To test the disparity between the predicted results and experimental errors that occur using a particular register length, TOF's were calculated using different precisions.

Fig. 3 compares the error bound given by (13) to the actual error that occurred when TOF was approximated using both first-degree and second-degree difference equations. The situation tested was one that matched conditions we used to acquire synthetic-aperture data and to generate synthetic-focus images. Errors given in Fig. 3 were expressed in multiples of the sampling interval, 20 ns (50-MHz sample rate). The sampling interval is the TOF separation between adjacent echo samples in backscatter memory. Errors shown in Fig. 3 are the worst-case values that occurred for all of the transducers in a 32-element, linear array. Element separation was 1.4 mm. The image was assumed to cover a 30×30 mm region, which was centered in front of the transducer array, at a minimum distance of 70 mm.

As expected, the actual TOF error always remained less than or equal to the predicted bound. For small register lengths, the actual error was much less than the predicted bound. As the size of the register was increased, however, the actual error approached the bound. For errors less than or equal to a single sample in backscatter memory, the experimental and predicted register lengths were separated by two or fewer bits. The small separation implies that (15) is a good indicator of the required precision, especially when the desired error is small. If the precision of the difference equation must be specified before the actual coefficients are known, then the bound on propagation distance given by (13) should be used to guarantee the accuracy of the TOF calculation.

VI. Image Generation Using Synthetic-Focus Techniques

A significant limitation of synthetic-focus imaging is the time required to produce an image. Almost all of the time needed to generate a synthetic-focus image is spent on one of three tasks: 1) TOF calculation, 2) retrieval of backscattered signals from memory, or 3) summation of backscattered values to define each pixel value. Image-generation time can be reduced by efficient algorithms for TOF calculation and by performing the operations within each of the major tasks in parallel.

Here, we present the results of generating synthetic-focus images on both serial and parallel machines. Specifically, images were generated on the Sun IPX serial processor and on the DAP 610 and DECmpp 12 000sx massively parallel processors. Algorithms were optimized for the different architectures of these machines to minimize the total image-generation time. Details of each of these algorithms can be found in [6]. Whenever TOF was determined using a difference equation, coefficients were scaled to yield locations into memory containing backscattered signals. Use of double precision (52 bits of mantissa plus a sign bit), floating-point registers provided at least 18 bits of error-free address (256 K locations) in backscatter memory over 512×512 images for second-degree approximations to TOF.

There are two obvious approaches to generating synthetic-focus images. One is to form and sum the subimages seen by each source-sensor pair in the transducer array. The other is to determine the contributions at each pixel from all source-sensor pairs in turn. Clearly, operations either for multiple source-sensor pairs or for multiple pixels can be performed in parallel.

A. SIMD Machines

The DAP 610 and the DECmpp are both single-instruction, multiple-data stream (SIMD) computers [12], i.e., a single instruction is performed on many sets of data at the same time. A SIMD computer contains a central control unit (array controller) with a large array of processors. When an instruction is issued to the array, each processor executes the instruction on data within its own memory. If there are N processors in the array, then N operations can be completed in a single instruction cycle. Many SIMD computers also contain a serial processor in addition to the processor array. If a segment of code cannot utilize the processor array efficiently, it may be faster to run it on this single, more powerful processor.

Both the DAP 610 and the DECmpp consisted of a host with an interface to an array controller and an array of processors. In each, the host, which was responsible for all I/O operations, could load the array controller with programs and data. In both systems, processing elements (PE's) of the array could also communicate directly with the host and with neighboring PE's in the same row or column.

The DAP 610 contained an array of 4096 PE's [13]. Each PE was a single-bit processor with 8 kilobytes of local memory. Memory in the PE array was subdivided into single-bit planes. A single-bit in each of the bit planes was dedicated to a given PE. During a memory retrieval, all of the PE's had to access memory from the same bit plane.

The DECmpp also contained an array of 4096 PE's [14]. Each PE contained a 32-b processor and 16 kilobytes of memory. A distinct advantage of the DECmpp over the DAP 610 was that its PE's could perform indirect addressing. Thus, during a memory cycle on the DECmpp, each PE could access its memory using a local pointer. In this way, PE's could retrieve data at addresses that differed from one PE to the next during the same instruction cycle.

B. Algorithms

The Sun IPX serial machine produced synthetic-focus images most rapidly when the contribution from each source-sensor pair in the transducer array was found one pair at a time for all pixels in the image. In other words, full images were formed for each source-sensor pair then added. On the other hand, both the DAP 610 and the DECmpp were most efficient when subimages were formed from all source-sensor pairs.

Because the elements of the DAP-610 array could not retrieve values from different memory locations at the same time, data retrieval and summation were performed by the host. TOF's, however, were calculated by the PE array. Image generation on the DAP 610 was optimized when its 4096-PE array calculated TOF's over 64×64 pixel subregions of the image. Each element in the array was responsible for calculating the TOF's associated with a single pixel using (1) and (2). Direct calculation of TOF using the square root of the sum of squares was used on the DAP 610 because communications and sample retrieval took one and two orders of magnitude longer, respectively. Direct calculation of TOF allowed us to quantify the limitations of the DAP 610 for synthetic-focus image generation. The use of a difference equation to find TOF's on the DAP 610 was not justified because it would have made an insignificant improvement in image-generation time.

Because of its ability to perform indirect addressing, the PE array of the DECmpp could handle retrieval from backscatter memory and data summation, as well as TOF calculation. In this case image generation time was minimized by determining the contribution from each source-sensor pair of transducers over a subregion of the image. A diagram of the algorithm

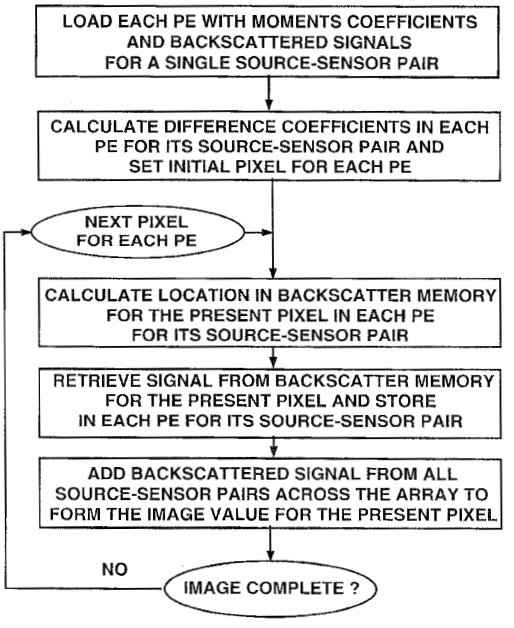

Fig. 4. Algorithm for synthetic-focus image generation using a difference equation to calculate TOF. This algorithm is suitable for an array processor with an indirect-addressing mode. PE is processing element.

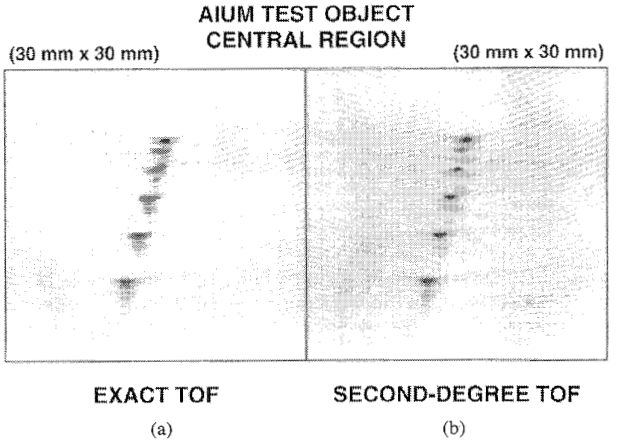

Fig. 5. 512×512 synthetic-focus images of the six central wires of the AIUM 100 mm test object in which all pixels are in focus on both transmission and reception. (a) Image generated using exact values for all TOF's. (b) Image generated using a second-degree polynomial approximation to all TOF's. TOF approximation was implemented as a difference equation. The wires are about 0.75 mm in diameter. The closest two wires are about 1 mm apart. The size of the area shown for each image is 30 mm $\times$ 30 mm.

is shown in Fig. 4. Data were loaded into the array so that a PE responsible for a particular source-sensor pair had the associated backscattered data and difference coefficients in its local memory. Size of the subimage generated in a given iteration depended on the number of elements in the ultrasonic transducer array used to acquire data. For example, for a 32-element array, there are 1024 source-sensor pairs. Because the array had 4096 PE's, it could calculate the contributions for all the source-sensor pairs over a 2×2 subimage in one iteration. By calculating 65 536 subimages, a 512×512 image was generated. The value of each pixel was found by global summation of backscattered signals. Global summation allows calculation of pixel values in $2\log_2(N)$ additions for an N-element transducer array. These summations occurred concurrently for all pixels in the subimage.

C. Test Conditions and TOF Errors

To test and compare the times required to generate synthetic-focus images using the complete dataset, images were formed of the six central wires of the American Institute of Ultrasound in Medicine (AIUM) 100-mm test object [15]. Synthetic-aperture data were collected for the complete dataset (all source-sensor pairs) from a custom Dapco 32-element, linear array of transducers with center frequencies of 3.5 MHz. Each of the 1024 backscattered signals contained 2024 samples. Backscattered signals were sampled at 50 MHz.

Synthetic-focus images were formed at an effective sample rate of 1/4 the actual sample rate. Oversampling by a factor of 4 reduced the need for interpolation during scan conversion [16], i.e., conversion from cylindrical to Cartesian coordinates, which is inherent in the TOF calculation. Because the backscattered signals were oversampled by a factor of four, 11 bits of address were required (9 for the 512 image size plus two for the oversampling factor). Two to the eleventh power is 2048, which is just slightly larger than the length of each backscattered signal (2024). Image size was set at 512×512 pixels. Any value for speed of sound could have been used, but a typical value for tissue, 1500 m/s, was used for this example. A 512×512 image from echoes acquired at an effective sample rate of 12.5 MHz covers a 30×30 mm region. This region was located at a minimum range of 50 mm from the array.

The error in a second-degree approximation to TOF over the image region was worst for transducer elements at the ends of the array. The maximum error was 90.4 ns, which corresponded to 68 μm or about 1.1 times the pixel separation of 60 μm. The average plus or minus the standard deviation for the TOF error of a second-degree polynomial for the end elements was -0.05 ± 13.2 ns. For the two elements closest to the propagation axis, it was -0.06 ± 1.95 ns. Formulation of the second-degree polynomial as a difference equation was done with register lengths that assured that no additional error was incurred due to the use of the difference equation. Fig. 5 compares an image formed using exact values for TOF to one formed using a second-degree approximation to TOF. The correlation coefficient for the two images was 0.999. The RMS value of pixel-by-pixel subtraction of the two images was 0.16% of the peak value of the exact-TOF image.

D. Generation Times

Generation of a 512×512 image on the Sun IPX using direct calculation of TOF (1) and (2) took 702 seconds. A second-degree difference equation for TOF reduced image generation time to 239 s. Table II shows the time it took each machine to generate a 512×512 image from 1024 source-sensor pairs. Timing measurements were done only for computations necessary for image-generation. Computations

TABLE II
GENERATION TIMES FOR A COMPLETE-DATASET, SYNTHETIC-FOCUS IMAGE
512 × 512 IMAGE, 32-ELEMENT TRANSDUCER ARRAY

Processor (Host)	Communications sec	TOF/Sum sec	Retrieval sec	Total sec
Sun IPX	-	-	-	239
DAP 610 (Sun4/110)	535	16.4[1]	1876	2428
DECmpp (DEC 5000/200)	8.8	6.0[2]	1.5	16.3

1) Direct calculation of TOF
2) Second-degree approximation to TOF

not strictly necessary for generating the image, such as disk input/output (I/O) or image display, are not included in these values.

The DAP 610 was the slowest of the machines tested. The need to retrieve backscattered data in a serial manner drastically increased the overall generation time. Although the time needed to calculate TOF was significantly less than for the serial machine, this savings was overwhelmed by the time needed to transfer the TOF's from the parallel processor to the host. To quantify this disparity, approximate measurements were made of the times the DAP 610 needed for communication, sample retrieval, and for calculation of TOF's and the sums of backscattered contributions. Communication and data retrieval took almost 99% of the total image-generation time. Attempts were made to keep the entire generation process on the processor array and eliminate most of the communication with the host. Because all processor elements are forced to retrieve data from the same address in a given instruction cycle, data retrieval had to be done in an almost serial manner. Some parallelism was accomplished by allowing processor elements which retrieved from the same memory location to do the access at the same time, but only a small fraction of the memory retrievals could take advantage of this parallelism. Since the processing elements were significantly slower than the host at performing the retrievals, this approach provided no improvement.

The ability to do sample retrieval and pixel summation in parallel gave the DECmpp a significant advantage over the other machines tested. This ability meant that all key activities took place in the PE array. No communication between the PE array and the host was needed during image formation. The only communication needed within the PE array itself was the communication between PE's required for global summation of backscattered signals to form the value of a pixel. Its indirect-addressing mode allowed the DECmpp to improve communication times by a factor of 60 over the DAP 610 and sample retrieval times by a factor of 1250. For the DECmpp, communication and sample retrieval occupy only 63% of the total image-generation time. The DECmpp did have the advantage of faster processors in the processor array than the DAP 610. This edge, however, was insignificant compared to the improvement gained by the use of the DECmpp's indirect-addressing mode.

VII. DISCUSSION

Representation of TOF with a difference equation reduced the time required to produce synthetic-focus images. For example, generation of a 512 × 512 image on a workstation (Sun IPX) was reduced from 702 to 239 seconds, i.e., by 66%. This reduction could be important in schemes in which images are generated iteratively under different assumptions about the medium being imaged. As a difference equation is used, however, recursive determination of the difference coefficients causes errors in those coefficients to increase. The number of bits needed to specify the error is a function of the degree of the approximation and the size of the image. The number of bits of error increases nearly logarithmically with image size. A bound on the number of bits over which error propagates was determined and used to set register length for TOF calculation using a difference equation. When acceptable errors were small, tests showed that the bound was only a few bits larger than actual errors encountered.

Register lengths needed to avoid errors in TOF values are much larger than the number of bits needed to represent the TOF itself for image sizes of interest in medical ultrasonic imaging. One method of reducing the required register lengths is to subdivide the image. For example, one set of initial difference coefficients could be calculated from the point common to the four subimages. TOF's could then be calculated from this point by using forward and backward difference equations. With this approach, the number of times a given difference equation is used is reduced. Consequently, both the error propagation distance and the length of the register required are also reduced.

Register lengths could also be reduced if the registers are designed to hold specific difference coefficients. The desired result, i.e., the TOF value (zeroth-order coefficient), requires more precision than the higher-order difference coefficients. The upper bits of the higher-order coefficients are zero, so that fewer bits are needed to represent those coefficients. Thus, the size of the registers holding each coefficient may be tailored to a given application. When the size of numbers being added is reduced, the size of the arithmetic unit adding them can be reduced as well.

The speed with which a parallel processor can generate a synthetic-focus image is dependent on its architecture. The use of indirect addressing to access local memory (used to store backscattered signals in our case) is essential if images are to be generated quickly. The DAP 610, whose PE's could not use pointers to their own memory, was even slower than the serial machine tested. Transferring TOF's to the host for retrieval of backscattered signals added significantly to the time needed for image reconstruction. Without an indirect-addressing mode,

a massively parallel processor cannot be used efficiently for synthetic-focus image generation.

The ability of the DECmpp to do indirect addressing in a parallel environment allowed it to perform the majority of operations in parallel and drastically reduce the number of instruction cycles needed to produce a synthetic-focus image. At 16.3 seconds per image, the DECmpp may prove to be a useful tool for studying methods of adaptively focusing images in response to assumptions about properties of the medium. For example, one application is to change the assumed pattern of variations in the speed of sound throughout the medium of interest until a "best-focused" image is produced. Such a process could not only produce a sharper image, but also may provide information about the local variation of the speed of sound within the medium of interest.

VIII. Conclusions

Generating synthetic-focus images from the complete dataset can be a very time consuming procedure. Image generation time for adaptive-focus schemes can be reduced by using difference equations to calculate TOF's. Knowing the precision needed by a difference equation is crucial to its accurate implementation. With adequate precision, a difference equation offers a fast and accurate method for calculating TOF's for synthetic-focus image production. By performing tasks associated with each pixel or with each transducer in parallel, synthetic-focus images can be generated significantly faster than can be done with a serial implementation. The improvement which can be achieved by a given parallel processor is dependent on its architecture. A massively parallel processor must have an indirect-addressing mode in order to efficiently generate synthetic-focus images.

References

[1] F. Duck, S. Johnson, J. Greenleaf, and W. Samayoa, "Digital image focussing in the near field of a sampled acoustic aperture," *Ultrason.*, vol. 15, pp. 83–88, 1977.

[2] A. Macovski, "Ultrasonic imaging using arrays." *Proc. IEEE*, vol. 67, pp. 484–495, 1979.

[3] O. T. von Ramm and S. W. Smith, "Beam steering with linear arrays," *IEEE Trans. Biomed. Eng.*, vol. BME-30, pp. 438–452, 1983.

[4] R. M. Arthur and S. R. Broadstone, "Imaging via Inversion of Ellipsoidal Projections of Solutions to the Linear Acoustic Wave Equation," *IEEE Trans. Med. Imag.*, vol. 8, pp. 89–95, 1989.

[5] ——, "The Effect of Background Velocity Variation on the Point-Spread Function of Ultrasonic Transducer Arrays," in *Proc. 1987 Ultrasonics Symp.*, IEEE no. 87CH242-7, 1987, vol. 2, pp. 947–950.

[6] D. G. Beetner, "Efficient Generation of Synthetic-Focus Ultrasonic Images Using Media-Dependent Time-of-Flight," master's thesis, Washington Univ., St. Louis, MO, 1994.

[7] S. R. Broadstone and R. M. Arthur, "An approach to real-time reflection tomography using the complete dataset," in *Proc. IEEE 1986 Ultrasonics Symp.*, no. 86CH2375-4, 1986, pp. 829–831.

[8] S. R. Broadstone and R. M. Arthur, "Time-of-flight approximation for medical ultrasonic imaging", *Acoustic Imaging*, vol 16. New York: Plenum, 1988, pp. 165–174.

[9] S. R. Broadstone and R. M. Arthur, "Determination of Time-of-Flight Surfaces Using the Method of Moments," *IEEE Trans. Med. Imag.*, vol. 10, pp. 173–179, 1991.

[10] S. Goldberg, *Introduction to Difference Equations.* New York: Wiley, 1963.

[11] G. Boole, *Calculus of Finite Differences* New York: Chelsea, 1958.

[12] J. L. Hennessy and D. A. Patterson, *Computer Architecture: A Quantitative Approach.* San Mateo, CA: Morgan Kaufmann, 1990.

[13] Active Memory Technology Inc, Irving, California, *Dap Series APAL Language*, 1988.

[14] Digital Equipment Corporation, Maynard, Massachusetts, *DECmpp System Overview Manual*, 1992.

[15] K. R. Erikson, P. L. Carson, and H. F. Stewart, "Field Evaluation of the AIUM Standard 100 mm Test Object", *Ultrasound Med.*, vol. 2, pp. 445–451, 1976.

[16] W. D. Richard and R. M. Arthur, "Real-Time Ultrasonic Scan Conversion via Linear Interpolation of Oversampled Vectors," *Ultrason. Imag.*, vol. 16, pp. 109–123, 1994.